



Research Article

Experimental Investigation on the Single Slope Desalination with Finned Pond for Four Different Saline Water Types

M. Yuvaperiyasamy ^a, N. Senthilkumar ^{a*}, B. Deepanraj ^b^a Saveetha School of Engineering, Saveetha Institute of Medical and Technical Sciences, Chennai, Tamil Nadu, India - 602105^b Department of Mechanical Engineering, College of Engineering, Prince Mohammad Bin Fahd University, Al Khobar, 31952, Saudi Arabia

PAPER INFO

Paper history:

Received 21 August 2023

Revised 21 November 2023A

Accepted 25 December 2023

Keywords:

Water Purification

Solar Still

Fins

Solar Energy

Desalination

Finned Solar Pond

A B S T R A C T

This experimental study investigates the performance of a single-slope solar desalination with a finned pond, considering varying glass cover angles, water depths, and the usage of sensible and latent heat materials for four different saline water types. Conventional solar stills (CSS) produce less distillate; therefore, some design changes were implemented by integrating a finned pond into the conventional solar still (CSS-FP). Additionally, paraffin wax and bricks were placed inside the solar still to enhance thermal storage capacity. The solar still is constructed with galvanized steel for the base and side walls, while the basin is covered with tempered glass. Thermal conductivity is improved by applying black paint on the sides. The finned pond enhances the heat absorption and distribution process, consequently increasing the evaporation rate within the still. The experiment was conducted in Pongalur, Tamil Nadu, India (10.9729° N, 77.3698° E). The maximum distillate production was achieved at a 35° glass cover angle and a 7 cm water depth. Desalination was performed on four saline liquids: bore water (BW), seawater (SW), leather industry wastewater (LW), and plastic industry wastewater (PW). BW exhibited the highest yield due to its lower density and salinity. Chemical analysis of the desalinated water suggests its suitability for home use. Economic research reveals a payback period of 230 days, confirming the financial feasibility of the solar still. Hence, it is concluded that the proposed CSS-FP can increase productivity compared to the CSS under different conditions.

<https://doi.org/10.30501/jree.2024.411088.1651>

1. INTRODUCTION

The contemporary demand for fresh water is substantial, driven by the escalating pollution in our modern lives. Addressing this challenge, water reclamation emerges as a potential solution. Various methods exist for converting seawater and industrial water into usable forms (Narayanan et al., 2020; Kalankesh et al., 2019). The most straightforward and cost-effective technique involves harnessing solar energy for purification. Literature and practical examples highlight that the daily production of freshwater using the traditional single-slope solar water purification process needs enhancement (Mohammed et al., 2023; Borzuei et al., 2021).

The conventional solar still, operating on the principle of condensation with a single slope, is inexpensive and easy to implement (Rajasekaran & Murugavel, 2022). While the annual maintenance cost of solar desalination is economical, the current design limits significant productivity increases (Ramzy et al., 2023). Altering the solar still's architecture, however, offers the potential to improve the quality and quantity of distilled water for irrigation and drinking purposes. Researchers have proposed various designs, including the dual-slope solar purifier, stepper solar purifier, wick-type solar

purifier, and multistage solar purifier (Omara et al., 2021; Saleem et al., 2021).

Studies reveal that modifications like a plane plate collector in a single-basin solar water purifier can increase production by 52%. Additionally, flowing cool water between two glass covers enhances productivity in the double glass cover-single slope basin (Eltawil & Omara, 2014). The stepper design solar still exhibits increased water productivity, with a 20% boost when a reflector is incorporated (Essa et al., 2021). Recent innovations, such as fins, wicks, and other heat energy-storing materials, aim to enhance efficiency. A basin-type stepper solar still equipped with a wick, as demonstrated by Abdelgaied et al. (2021) and Younes et al. (2022), produces exceptionally pure water, outperforming basin-type systems. Moreover, a multi-basin solar still has been found to boost thermal storage and overall performance (Hansen et al., 2015; Mohammed et al., 2022).

The effectiveness of different basin layouts, including the use of pin fins, steel wool fibers, and phase change material, was evaluated in terms of output, cost-effectiveness, and environmental sustainability. The steel wool fiber solar still basin outperformed other designs (Yousef & Hassan, 2019). Transparent walls made of naturally porous materials like

Please cite this article as: No need to fill, this section will be filled by the journal..



charcoal and coco peat also demonstrated enhanced productivity levels (Mande & Manickam, 2018). Various modifications, such as using copper oxide nano-coated absorber plates and polyvinyl alcohol sponges, were explored in research. The solar still with an absorber plate coated with copper oxide nanoparticles exhibited the highest efficiency at 53% (Arunkumar et al., 2019). The impact of Fresnel lenses on a solar still's efficiency revealed an impressive 84.7% boost compared to conventional methods (Mu et al., 2019).

Kabeel et al. (2019) investigated the impact of composite material on solar still heat storage, showing a 38% improvement in energy efficiency compared to stills without phase change material. The cost per litre of water produced by the composite material solar still was 27% less than that of an alternative solar still. Sharshir et al. (2020) explored the use of a metal-chip wick, finding that a copper basin with a copper chip wick had the best thermal efficiency at 60.98%. Additionally, research by Sahoo and Subudhi (2019) indicated that jute fabric, internal reflectors, and changes in glass inclination angle significantly influenced solar still efficiency, showing a 72.18% improvement compared to traditional solar stills.

From the existing literature review, it is evident that further research is needed to enhance the efficiency of a single-slope solar desalination system for increased productivity, utilizing different variants of solar stills and design changes. The objective of this study is to develop a novel distillation method using a single-basin solar still integrated with a solar pond. This study considers adjusting the depth of the water, the angle of the glass cover, and the presence of sensible and latent heat materials. Various water sources, including sea water, bore water, leather, and plastic industrial waste water, are explored for treatment and reuse of the distillate. Experimental investigations were conducted in May 2023 on a hot sunny day. Finally, the outcomes of the experiments from the proposed system are contrasted with those obtained using a traditional solar still.

2. EXPERIMENTAL SETUP AND EXPERIMENTAL PROCEDURE

2.1 Conventional solar still

A schematic representation of a typical Conventional Solar Still (CSS) is shown in Figure 1. The components of a typical solar still include pipe connections, thermometers, a solar still, and a storage tank. The galvanized iron solar still basin is 0.12 meters deep and 2 mm thick. To maximize sunlight absorption, the still basin was coated with dull black from top to bottom. The solar still basin is housed inside a wooden box that is 1.2 m × 1.2 m × 0.19 m wide and 0.1 m high. The interior of the wooden box was painted white to maximize the quantity of sunlight that reached the water's surface. To prevent heat loss, sawdust is placed between the still basin and the wooden box. The 5 mm thick glass cover on top of the wooden box is placed at a 35° angle in Pongalur at the latitude of (10.9729° N, 77.3698° E). The 35° slope refers to the angle at which the glass cover is inclined to maximize sunlight exposure (Yuvaperiyasamy et al., 2023a). In this experiment, the critical glass cover angle is determined by varying the glass cover angle from 35, 45, and 50°.

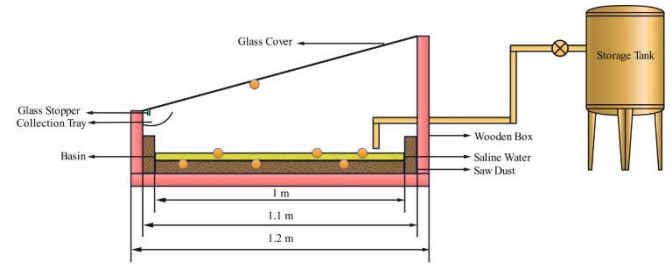


Figure 1. Conventional solar still (Yuvaperiyasamy et al., 2023a)

2.2 Conventional solar still with finned solar pond (GSS-FP)

In this research, a novel Compact Solar Still with a finned pond (CSS-FP) has been developed, and its performance is compared with that of a conventional Compact Solar Still (CSS). Solar ponds, being thermal devices that absorb and store solar energy for later use, play a crucial role in sustainable energy solutions. The mini-solar pool used in the study has top and bottom surface areas of 0.63 and 0.07 m², respectively, with a 0.3 m axial height. This design results in three distinct zones: the Lower Convective Zone (LCZ), Non-Convective Zone (NCZ), and Upper Convective Zone (UCZ).

To enhance the solar pond's efficiency, four rectangular fins, each measuring 200 mm in length, 50 mm in width, and 2 mm in thickness, were strategically placed at the base. The introduction of fins serves to augment the still's capacity to absorb and distribute heat effectively. The improved heat transfer and distribution contribute to an elevated evaporation rate, consequently leading to increased distillate production. Importantly, the incorporation of fins in the solar pond significantly enhances the desalination efficiency of the system, resulting in higher productivity for obtaining fresh water from saline sources.

Figure 2 illustrates the suggested CSS-FP, while Figure 3 provides a schematic and 3D representation of the proposed setup, comprising a saline water tank, finned solar pond, and Solar still. These findings not only contribute to the advancement of solar pond technology but also underscore the potential of CSS-FP as an efficient and sustainable solution for desalination and fresh water production.

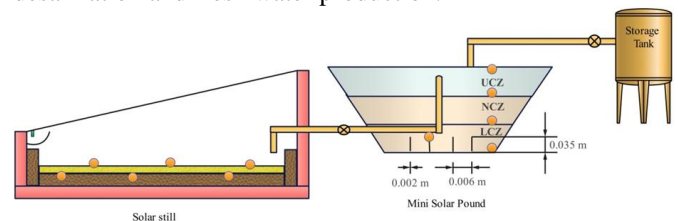


Figure 2. Conventional solar still with finned pond and still (Yuvaperiyasamy et al., 2023a)

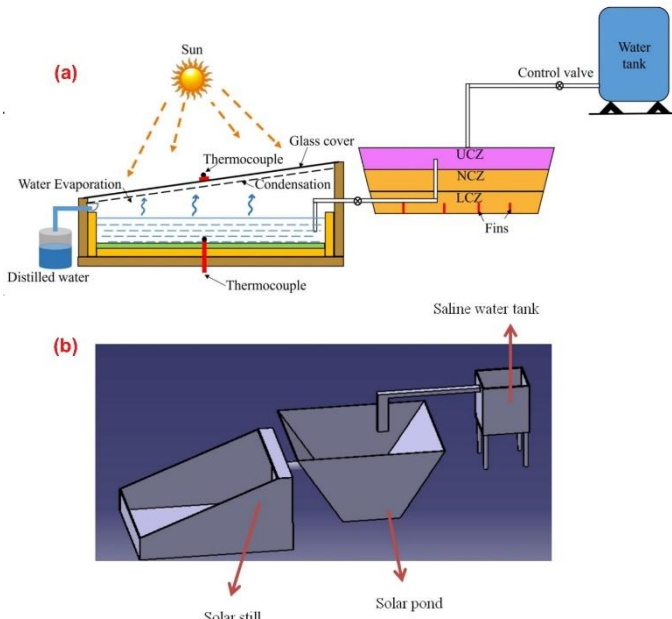


Figure 3. (a) Schematic diagram of the proposed setup (b) 3D diagram of the proposed setup

2.3 Experimental procedure

The desalination process begins when saline water is subjected to solar radiation, causing it to heat up. As the temperature rises, the water in the basin undergoes vaporization, and the resulting vapor condenses on the glass cover. The condensed water is then collected in a trough positioned at the base of the glass cover. This experiment, conducted in Pongalur, Tamil Nadu, India, in May 2023, meticulously measured various parameters such as wind speed, solar radiation, basin plate temperature, and water characteristics, including distilled water. Additionally, the angle of the glass cover was considered on an hourly basis.

The experimentation encompassed both traditional methods and the recently developed CSS-FP (Solar Still using Finned Plate). Hourly outputs were systematically quantified for each setup. The CSS-FP performance was evaluated under diverse conditions, including variations in wastewater depth (h), adjustments to the glass cover inclination angle (θ), the incorporation of sensible and latent heat materials such as paraffinized wax and bricks, and changes in the type of liquid to be purified. The latter included bore water, seawater, wastewater from the plastic industry, and wastewater from the leather industry.

2.4 Measuring instruments and error analysis

The solar power meter TES 1333R measures the sun's intensity, with a range of $0-2500 \text{ W/m}^2$ and an accuracy of $\pm 1 \text{ W/m}^2$. The measurement of air velocity is conducted using a cup-type anemometer, which has a precision of $\pm 0.1 \text{ m/s}$ and a measurement range spanning from 0 to 45 m/s . K-type thermocouples are used for temperature monitoring, ranging from 0 to 100°C . These thermocouples exhibit an accuracy level of $\pm 1^\circ\text{C}$. The water depth inside the solar still was quantified using a calibrated scale possessing a precision of $\pm 0.1 \text{ cm}$ (Yuvaperiyasamy et al., 2023b; Younes et al., 2021). Table 1 shows instruments used in the experiment.

Table 1. Instrument range, error and device accuracy

Instrument	Precision	Range	Inaccuracy (%)
Anemometer	$\pm 0.1 \text{ m/s}$	$0-45 \text{ m/s}$	10
Thermocouple	$\pm 1^\circ\text{C}$	$0-100^\circ\text{C}$	0.25
Solar power meter	$\pm 1 \text{ W/m}^2$	$0-2500 \text{ W/m}^2$	2.5
Beaker	$\pm 10 \text{ mL}$	$0-1000 \text{ mL}$	10

3. Result and Discussion

3.1. Impact of temperature and solar radiation on performance of CSS & CSS-FP

The temperatures of the glass cover, basin water, and solar radiation are monitored hourly in both the CSS and CSS-FP systems. Figure 4 vividly portrays the variation in solar radiation corresponding to the local time zone, with the maximum solar radiation peaking at 1000 W/m^2 around 14 hours. The impact of solar intensity on the glass cover and basin water temperatures is evident in Figure 5, showcasing the dynamic changes over time. Thermocouples, strategically placed in the glass cover and water basin at the midpoint, capture these fluctuations. At 14 hours, the basin water's highest temperature is noted at 64°C for CSS-FP and 60°C for CSS. This temperature surge correlates with increased solar radiation, underscoring its influence on the system.

Moreover, the temperature trends reveal that solar radiation significantly influences the glass and water temperatures in both CSS-FP and CSS. The collected data provides profound insights into the thermal dynamics of these designs. Notably, CSS-FP exhibits advantages in temperature regulation and overall performance, as depicted in figures 4 and 5. To comprehend the thermal dynamics comprehensively, thermocouples are immersed at various depths (LCZ, NCZ, and UCZ) in the pond, providing a detailed analysis of temperature variations across the water column. Evaporation intensity, a crucial parameter, is evaluated using evaporation sensors on the glass surface, considering temperature and humidity differences with the surrounding air. The solar radiation intensity, recorded by a pyranometer above the solar still, is a pivotal metric for assessing the system's efficiency and adaptability to different environmental conditions. The meticulous measurements at specific locations contribute to a nuanced understanding of temporal and spatial variations, enhancing the evaluation of the solar still's overall performance (Singh et al., 2023; Abdullah et al., 2022).

This comprehensive monitoring and analysis underscore the potential of CSS-FP in not only harnessing solar energy efficiently but also adapting to diverse environmental conditions, offering valuable insights for advancements in solar still technology. References have not been provided in the given text; kindly share them to complete the proofreading process accurately.

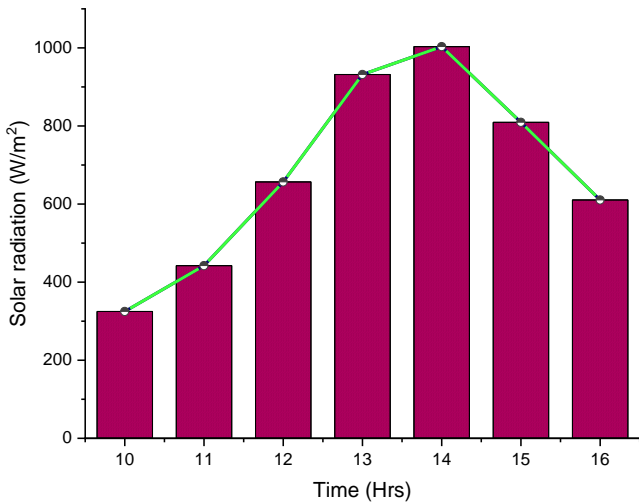


Figure 4. Solar radiation changes with time

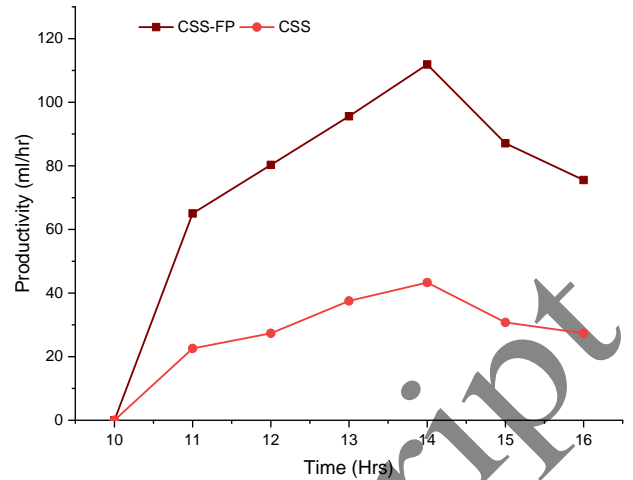


Figure 6. Hourly productivity of the water between the CSS and CSS-FP

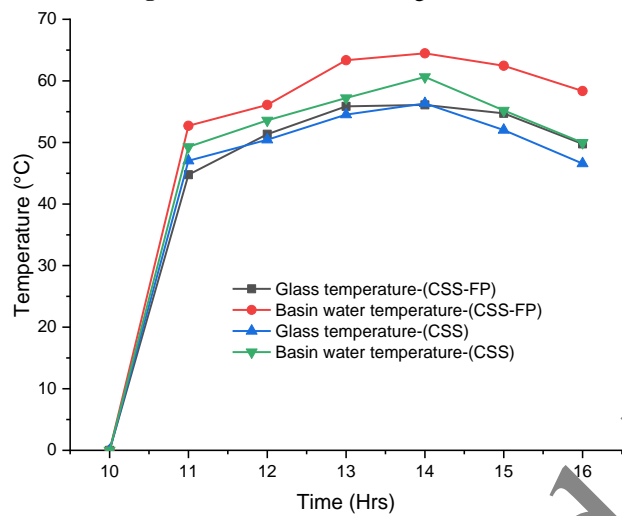


Figure 5. Variation of glass and basin temperature of CSS and CSS-FP

3.3 Performance of CSS-FP on different water depths

Figure 7 illustrates the water output of the CSS-FP at different water depths when utilizing bore water as the saline source. The experiment's objective is to ascertain the optimal water depth for the CSS-FP, with depths of 7 cm, 14 cm, and 21 cm tested, while maintaining a consistent inclination angle of the glass cover at 35°. The results reveal a discernible pattern: solar production decreases with an increase in water depth. The highest desalination yield is observed at the shallowest water depth of 7 cm. Several factors contribute to achieving the maximum yield at this depth. A key factor is the reduced water depth in the basin. With a lower water depth, a smaller mass of water is exposed to solar radiation, resulting in faster heating and subsequent vaporization. Consequently, the CSS-FP achieves a higher rate of water vapor production, enhancing desalination productivity. Furthermore, the smaller volume of water in the basin contributes to a higher specific heat capacity of water. This implies that a relatively minor amount of energy is needed to heat the water for vaporization. Consequently, the solar still operates more efficiently at the 7 cm water depth compared to deeper levels.

3.2 Hourly productivity comparison between GSS and CSS-FP

The hourly shifts in purified water output for CSS and CSS-FP are depicted in Figure 6. The maximum desalination yield was 112 ml/h for CSS-FP and 44 ml/h for CSS. The experiment uses bore water as the saline water in both solar still setups, with a water depth of 7 cm and a static glass cover angle of 35°. The results show that the desalinated water produced is initially low and gradually increases with time. Water takes time to warm up and alter into water vapor. The temperature of the water rises as the solar radiation intensity increases, resulting in a quicker rate of water vaporization and a higher output of desalinated water. The maximum yield of desalinated water is attained, suggesting that the solar stills perform optimally when solar radiation is at its mid-day optimum. As a result, as solar energy falls in the late afternoon, desalinated water output diminishes progressively. According to the trial results, CSS-FP is more productive than CSS still. The CSS-FP produces roughly twice as much desalinated water as the CSS. This significant difference in productivity underlines the CSS-FP design's superiority, proving its potential as a more efficient and effective approach to desalination.

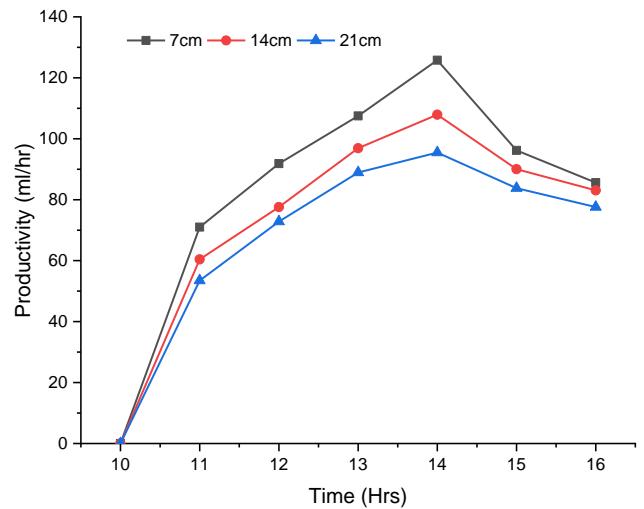


Figure 7. Hourly productivity of CSS-FP at different water depths

3.4 Performance of CSS-FP on different glass cover inclination

The desalination yield can be significantly influenced by adjusting the glass cover angle (θ) in the CSS-FP, as described in Figure 8. This experiment's glass cover angle varies at three different settings: 35, 45, and 50°. Precision inclinometers and adjustable supports were used to achieve the desired angles. The angles were precisely controlled and observed to keep the system's dimensions and volume constant during the experiment. This was done to isolate the effect of glass cover inclination on CSS-FP efficiency. Bore water is utilized as the water source, and a consistent depth of 7 cm is maintained throughout the experiment. Figure 8 displays the hourly-based purification yield achieved at several glass angles in the CSS-FP. The outcomes demonstrate that the inclination angle of the glass cover has a notable impact on the overall desalination yield productivity. Upon analysis, it becomes apparent that the CSS-FP achieves the maximum distillate when the glass cover is inclined at 35°. At this specific angle, the solar still exhibits the most efficient efficiency in terms of desalination productivity.

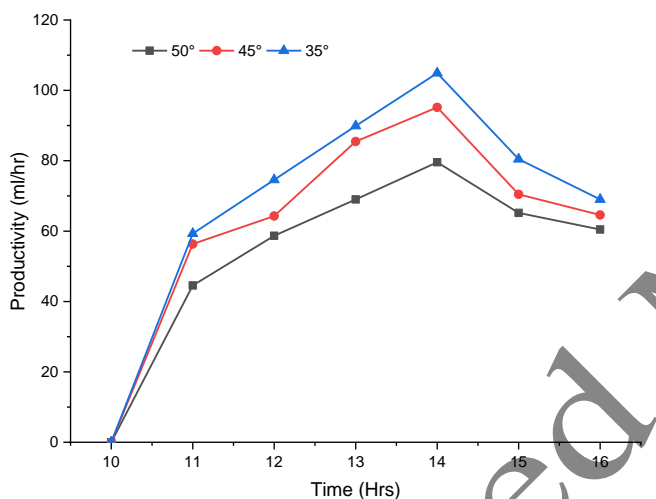


Figure 8. Hourly productivity of CSS-FP at different glass cover angles

3.5 Performance of CSS-FP on addition of latent and sensible heat materials

To improve the heat retention and storage capacity within the basin of the CSS-FP, a combination of latent and sensible materials, specifically brick and paraffin wax, is introduced as separate thermal storage components. The experiment commences by placing half-filled paraffin wax in a smaller stainless steel container within the solar still area. This design allows the paraffin wax to absorb heat from the rising base water temperature, leading to its melting and consequently adding more heat to the salty water. The absorption and melting of paraffin wax enhance thermal conductivity and vaporization within the solar still, contributing to the overall desalination process.

Following the experimentation with paraffin wax, bricks are introduced into the saline water area. The bricks function as heat absorbers, extracting thermal energy from the salty water during the experiment. Over time, these bricks release the stored heat, further aiding in the desalination process. Throughout the investigation, the CSS-FP is consistently maintained at a fixed angle of 35°, while the saline water level

is kept at a constant 7 cm. As depicted in Figure 9, the incorporation of both sensible and latent heat materials significantly amplifies the productivity of desalinated water. Notably, the desalination process exhibits a distinct tendency, with water temperature peaking in the late afternoon. It is interesting to observe that including bricks in the CSS-FP structure results in a larger yield compared to using only paraffin wax.

The combined impact of these thermal storage materials enhances the overall performance of the solar still, fostering higher productivity and improved efficiency in water vaporization. These findings offer valuable insights into the advantages of employing both sensible and latent heat materials as heat storage components in solar desalination systems.

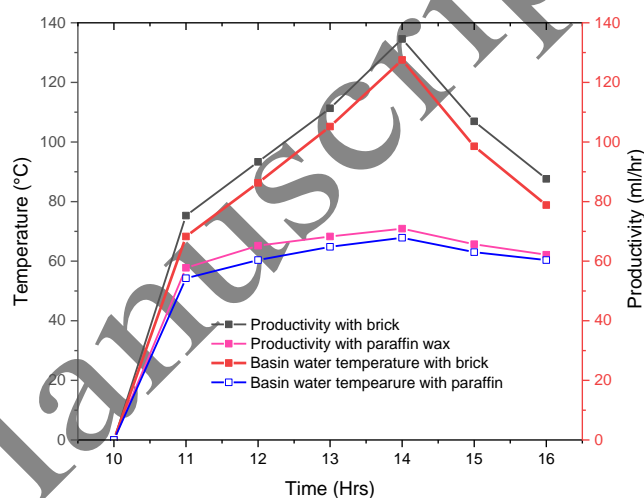


Figure 9. Hourly productivity of CSS-FP on addition of latent and sensible heat materials

3.6 Performance of the CSS-FP for Different Saline Water types

The desalination procedure examined in this study utilizes four distinct types of saline water in the CSS-FP. The four saline water sources investigated are bore water (BW), wastewater from the plastic industry (PW), seawater (SW), and Leather industry wastewater (LW) from the leather industry. The desalination yields obtained for each saline water type are visually represented in Figure 10. Upon analysis, it is evident that the CSS-FP demonstrates the most significant yield of desalinated water when bore water is employed as the saline source. This superior performance with bore water can be attributed to its relatively lower density and salinity compared to the other water types, rendering it more conducive to desalination. The system's efficiency exhibits an increase with higher solar radiation levels, facilitating greater heat generation and evaporation. Conversely, the efficiency of the system may decline during periods of low or intermittent solar radiation, leading to reduced energy availability for the desalination process. It is noteworthy that for the solar desalination system to operate consistently and effectively throughout the day and across seasons, the crucial factor is the fluctuation in hourly solar radiation patterns (Kumaravel et al., 2023).

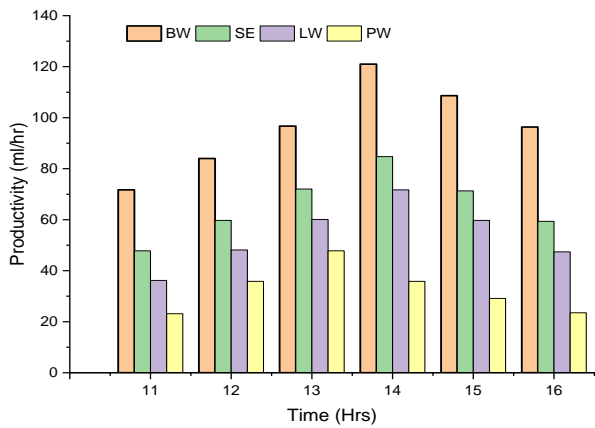


Figure 10. Hourly productivity of CSS-FP for different saline water

3.7 Efficiency of the CSS-FP for different saline water

The efficiency of the CSS-FP for different saline water types is shown in Figure 11.

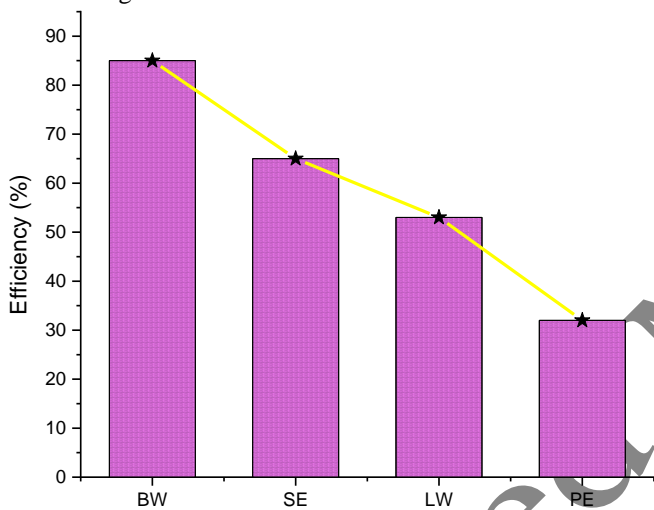


Figure 11. Efficiency of CSS-FP for different saline water types

Borewell water (BW) boasts an impressive efficiency rate of 85%, underscoring its efficacy in purifying groundwater from bore wells. In comparison, sea water (SE) exhibits a conversion efficacy of 65%, positioning it as a viable option for desalination and the production of potable water. The wastewater treatment system for the leather industry

demonstrates a moderate capacity, with an efficacy of 53%, showcasing its capability to cleanse effluent. However, the treatment of plastic industry wastewater (PE) lags behind with the least efficiency at 32%, revealing limitations in its ability to purify plastic industry effluent.

3.8 Chemical Examination of Different Saline Water

The experiment took place in Pongalur, Tamil Nadu, India, under the auspices of the Tamil Nadu Water Supply and Drainage Board. Table 2 details the outcomes of desalinating four distinct saline water types, providing insights into the yields for each. Additionally, a chemical analysis of the desalinated water was conducted, affirming that its quality adheres to domestic usage norms (Khedmati and Shafiq, 2020). This study holds significance as it illuminates the potential use of desalinated water for household needs, offering a pragmatic alternative for addressing water scarcity and ensuring a clean water supply in regions with limited freshwater resources. The distilled water produced by the proposed system finds utility in various applications, such as sterilizing lead-acid batteries, medical equipment, car cooling systems, and other equipment susceptible to mineral build-up.

3.9 Economic Analysis

Table 3 illustrates a comprehensive economic analysis of the proposed solar still, incorporating the calculation of the payback time. The payback period is determined by dividing the fabrication cost by the net profit, representing the disparity between the cost of water production and maintenance expenditures (Ahangar dharabi et al., 2022). The economic scrutiny reveals a 230-day payback period for the solar still. This signifies that the initial investment in solar technology can be recouped within a relatively short timeframe, rendering it not only financially advantageous but also economically feasible.

The data suggests that solar energy mitigates the operational expenses associated with water desalination, providing a cost-effective and enduring solution to challenges linked with water scarcity. The favorable payback period of solar still technologies underscores their potential economic advantages, advocating for their broader implementation to support water sustainability and establish a dependable source of clean water in regions grappling with water crises.

Table 2. Chemical examination of saline water

S. No	Property / Ions	Permissible limit	BW	Desalinated BW	SW	Desalinated SW	LW	Desalinated LW	PW	Desalinated PW
1	Turbidity	5	2	2	3	2	150	3	220	2
2	Alkalinity	600	340	120	260	122	900	190	1200	420
3	Hardness (mg/L)	600	450	120	8700	310	1200	310	5100	540
4	Na (mg/L)	-	210	120	5400	370	880	540	4500	310
5	Mg (mg/L)	100	53	17	1700	33	120	32	1008	70
6	K (mg/L)	-	20	7	420	25	17	9	220	22
7	Dissolved solids (mg/L)	2000	650	310	33230	1780	5430	1890	23100	1728
8	Ca (mg/L)	200	86	30	490	70	430	70	420	75

9	Fe (mg/L)	0.3	0	0	0.1	0	14	0.2	20	0
10	NH ₃ (mg/L)	0.5	0	0	0	0	7.8	0	12.8	0.18
11	NO ₃ (mg/L)	45	4	0	14	0	28	5	24	10
12	CL (mg/L)	1000	340	220	15500	650	2200	920	9200	550
13	F(mg/L)	1.5	0.4	0.2	1.6	0.4	1.6	0.6	1.6	1
14	SO ₄ (mg/L)	400	30	25	1430	43	144	84	650	50
15	PO ₄ (mg/L)	-	0	0	0	0	2	0.4	4	0.8
16	NO ₃ (mg/L)	45	4	0	14	0	28	5	25	10
17	O ₂ (mg/L)	-	0.7	0.6	1.1	0.5	1.02	0.5	1.61	0.70

Table 3. Economic analysis of the proposed system

S. No	Fabrication cost (Rs)	Maintenance per day (Rs)	Purified water cost (Rs)	Net Profit Per day (Rs)	Payback Period
CSS-FP	4500	0.5	20	19.5	230 days

3.10 Technical, economical and environmental comparison of CSS-FP with CSS

Table 4 shows the technical and economical comparison between the proposed still and conventional solar still.

Table 4. Comparison of CSS-FP and CSS in terms of technical and economical aspects

S. No	Productivity (ml/hr)	Payback period (Days)
CSS-FP	112 ml/hr	230
CSS	44 ml/hr	350

The CSS-FP solar still demonstrates higher productivity, yielding 112 ml/hr of freshwater, compared to the CSS solar still, which has a lower output of 44 ml/hr. The payback period is the duration required for the initial investment in the solar still to be recovered through savings in freshwater production. In this context, CSS-FP demonstrates a payback period of 230 days, signifying that the initial investment is recuperated in roughly 230 days. In contrast, the CSS solar still exhibits a payback period of 350 days, indicating a comparatively longer duration for recuperating the initial investment through freshwater conservation.

When considering the environmental aspect, the finned pond in the conventional solar still offers notable environmental benefits compared to a standard solar still. By incorporating enhanced heat transfer mechanisms through fins, energy consumption is reduced, resulting in decreased carbon emissions. In contrast to traditional stills, the enhanced design recirculates brine to minimize water waste and encourage water conservation. Moreover, the improved solar still offers a more sustainable approach to obtaining freshwater, especially in dry areas. This makes it a viable option for addressing the environmental consequences of water scarcity and conventional solar stills.

4. CONCLUSIONS

The CSS-FP can achieve a maximum productivity of 112 ml/h, surpassing that of CSS. The still's productivity is influenced by

water depth, with the maximum of 125 ml/h observed at a 7 cm depth. Additionally, the inclination angle impacts the productivity of both CSS-FP and CSS, with the highest productivity achieved at a 35° inclination. This research meticulously examined and analyzed the performance and financial viability of a CSS-FP for water desalination.

The effectiveness, productivity, and economic viability of solar stills were comprehensively evaluated through a series of experiments and studies. According to the findings, the CSS-FP exhibits excellent potential in addressing water scarcity challenges in regions with limited freshwater sources. In terms of desalination productivity, experimental results indicate that the CSS-FP outperforms the CSS. The use of tempered glass and enhanced heat conductivity from the black paint coating accelerates water vaporization, resulting in increased desalinated water yields.

Incorporating sensible and latent heat components such as paraffin wax and bricks, which improve thermal storage, further enhances water output. A comparative investigation shows a 9.20% increase in productivity by adding bricks. The hourly variation in desalination output illustrates how solar radiation strength, water depth, and glass cover angle affect the still's performance. After identifying the optimal water depth and glass cover angle, the study examines their effects on desalination production.

Chemical analysis of the desalinated water confirms its suitability for residential use, establishing the CSS-FP as a reliable source of clean water. The economic study's favorable payback period of 230 days indicates that the solar investment can be quickly reimbursed. Lower operational expenses due to solar energy use enhance the economic viability and popularity of this sustainable option. Consequently, based on the study's findings, the proposed CSS-FP can confidently be used for desalination of various liquids such as bore water, industrial wastewater, seawater, and plastic wastewater.

5. ACKNOWLEDGEMENT

The authors would like to convey their deepest gratitude to the Saveetha School of Engineering, Saveetha Institute of Medical and Technical Sciences, Chennai, Tamil Nadu, India for

providing the research facilities and for their invaluable support.

REFERENCES

1. Abdelgaied, M., Zakaria, Y., Kabeel, A. E., & Essa, F. A. (2021). Improving the tubular solar still performance using square and circular hollow fins with phase change materials. *Journal of Energy Storage*, 38, 102564. <https://doi.org/10.1016/j.est.2021.102564>
2. Abdullah, A. S., Omara, Z. M., Bacha, H. B., & Younes, M. M. (2022). Employing convex shape absorber for enhancing the performance of solar still desalination system. *Journal of Energy Storage*, 47, 103573. <https://doi.org/10.1016/j.est.2021.103573>
3. Ahangar Darabi, M., Pasha, G., Ebrahimpour, B., Guodarzi, A. M., Morshedsolouk, F., Habibnejad Roshan, H., & Shafaghat, R. (2022). Experimental investigation of a novel single-slope tilted wick solar still with an affordable channelled absorber sheet, an external condenser, and a reflector. *Solar Energy*, 241, 650–659. <https://doi.org/10.1016/j.solener.2022.06.020>
4. Arunkumar, T., Murugesan, D., Raj, K., Denkenberger, D., Viswanathan, C., Rufuss, D. D. W., & Velraj, R. (2019). Effect of nano-coated CuO absorbers with PVA sponges in solar water desalting system. *Applied Thermal Engineering*, 148, 1416–1424. <https://doi.org/10.1016/j.applthermaleng.2018.10.129>
5. Borzuei, D., Moosavian, S. F., Ahmadi, A., Ahmadi, R., & Bagherzadeh, K. (2021). An experimental and analytical study of influential parameters of parabolic trough solar collector. *Journal of Renewable Energy and Environment*, 8(4), 52–66. <https://doi.org/10.30501/jree.2021.261647.1172>
6. Eltawil, M. A., & Omara, Z. M. (2014). Enhancing the solar still performance using solar photovoltaic, flat plate collector and hot air. *Desalination*, 349, 1–9. <https://doi.org/10.1016/j.desal.2014.06.021>
7. Essa, F. A., Abou-Taleb, F. S., & Diab, M. R. (2021). Experimental investigation of vertical solar still with rotating discs. *Energy Sources, Part A: Recovery, Utilization, and Environmental Effects*, 1–21. <https://doi.org/10.1080/15567036.2021.1950238>
8. Hansen, R. S., Narayanan, C. S., & Murugavel, K. K. (2015). Performance analysis on inclined solar still with different new wick materials and wire mesh. *Desalination*, 358, 1–8. <https://doi.org/10.1016/j.desal.2014.12.006>
9. Kabeel, A. E., Abdelaziz, G. B., & El-Said, E. M. S. (2019). Experimental investigation of a solar still with composite material heat storage: Energy, exergy and economic analysis. *Journal of Cleaner Production*, 231, 21–34. <https://doi.org/10.1016/j.jclepro.2019.05.200>
10. Kalankesh, L. R., Zazouli, M. A., & Mansouri, A. (2019). Efficiency of Low-Pressure Reverses Osmosis (RO) in Desalination and TOC Removal from Caspian Seawater and Tajan River. *Journal of Renewable Energy and Environment*, 6(3), 32–37. <https://doi.org/10.30501/jree.2019.100262>
11. Khedmati, A. R., & Shafii, M. B. (2020). Multi-Objective Optimization of the Humidification-Dehumidification Desalination System for Productivity and Size. *Journal of Renewable Energy and Environment*, 7(1), 1–11. <https://doi.org/10.30501/jree.2020.104062>
12. Kumaravel, S., MeenakshiSundaram, N., & Bharathiraja, G. (2023). Thermal Investigation of Single slope solar still by using Energy Storage Material. *Journal of Renewable Energy and Environment*. <https://doi.org/10.30501/jree.2023.376724.1518>
13. Mande, A. B., & Manickam, P. (2018). Enhanced solar still productivity using transparent walls with an integral trough and organic porous absorber material. *International Journal of Green Energy*, 16(3), 211–227. <https://doi.org/10.1080/15435075.2018.1549995>
14. Mohammed, A. H., Attalla, M., & Shmroukh, A. N. (2022). Comparative study on the performance of solar still equipped with local clay as an energy storage material. *Environmental Science and Pollution Research*, 29(49), 74998–75012. <https://doi.org/10.1007/s11356-022-21095-z>
15. Mohammed, A. H., Shmroukh, A. N., Ghazaly, N. M., & Kabeel, A. E. (2023). Active solar still with solar concentrating systems. *Review. Journal of Thermal Analysis and Calorimetry*, 148(17), 8777–8792. <https://doi.org/10.1007/s10973-023-12285-z>
16. Mu, L., Xu, X., Williams, T., Debroux, C., Gomez, R. C., Park, Y. H., Wang, H., Kota, K., Xu, P., & Kuravi, S. (2019). Enhancing the performance of a single-basin single-slope solar still by using Fresnel lens: Experimental study. *Journal of Cleaner Production*, 239, 118094. <https://doi.org/10.1016/j.jclepro.2019.118094>
17. Narayanan, S. S., Yadav, A., & Khaled, M. N. (2020). A concise review on performance improvement of solar stills. *SN Applied Sciences*, 2(3). <https://doi.org/10.1007/s42452-020-2291-5>
18. Omara, Z. M., Abdullah, A. S., Essa, F. A., & Younes, M. M. (2021). Performance evaluation of a vertical rotating wick solar still. *Process Safety and Environmental Protection*, 148, 796–804. <https://doi.org/10.1016/j.psep.2021.02.004>
19. Rajasekaran, A. K., & Murugavel Kulandaivelu, K. (2022). Performance comparison of solar still with inbuilt condenser and agitator over conventional solar still with energy and exergy analysis. *Environmental Science and Pollution Research*, 29(55), 83378–83388. <https://doi.org/10.1007/s11356-022-21466-6>
20. Ramzy, K., Abdelgaleel, M., Kabeel, A. E., & Mosalam, H. (2023). Performance of a single slope solar still using different porous absorbing materials: an experimental approach. *Environmental Science and Pollution Research*, 30(28), 72398–72414. <https://doi.org/10.1007/s11356-023-27465-5>
21. Sahoo, B., & Subudhi, C. (2019). Performance enhancement of solar still by using reflectors-jute cloth-improved glass angle. *The Journal of Engineering Research [TJER]*, 16(1), 1. <https://doi.org/10.24200/tjer.vol16iss1pp1-10>
22. Saleem, R. N., Khan, S. N., Khan, H. M. S., & Nasir, A. (2021). Productivity comparison of conventional and single slope solar still with internal reflectors: an overview. *Earth Sciences Pakistan*, 5(1), 16–19. <https://doi.org/10.26480/esp.01.2021.16.19>
23. Sharshir, S. W., Peng, G., Elsheikh, A. H., Eltawil, M. A., Elkadeem, M. R., Dai, H., Zang, J., & Yang, N. (2020). Influence of basin metals and novel wick-metal chips pad on the thermal performance of solar desalination process. *Journal of Cleaner Production*, 248, 119224. <https://doi.org/10.1016/j.jclepro.2019.119224>
24. Singh, B. K., Ramji, C., Ganeshan, P., Mohanavel, V., Balasundaram, T., Kumar, V. V., Balasubramanian, B., Ramshankar, P., Ramesh, A., & Thanappan, S. (2023). Performance Analysis of Solar Still by Using Octagonal-Pyramid Shape in the Solar Desalination Techniques. *International Journal of Photoenergy*, 2023, 1–9. <https://doi.org/10.1155/2023/4705193>
25. Younes, M. M., Abdullah, A. S., Essa, F. A., Omara, Z. M., & Amro, M. I. (2021). Enhancing the wick solar still performance using half barrel and corrugated absorbers. *Process Safety and Environmental Protection*, 150, 440–452. <https://doi.org/10.1016/j.psep.2021.04.036>
26. Younes, M. M., Abdullah, A. S., Omara, Z. M., & Essa, F. A. (2022). Enhancement of discs' solar still performance using thermal energy storage unit and reflectors: An experimental approach. *Alexandria Engineering Journal*, 61(10), 7477–7487.
27. Yousef, M. S., & Hassan, H. (2019). Assessment of different passive solar stills via exergoeconomic, exergoenvironmental, and exergoenvironmental approaches: A comparative study. *Solar Energy*, 182, 316–331. <https://doi.org/10.1016/j.solener.2019.02.042>
28. Yuvaperiyasamy, M., Senthilkumar, N., & Deepanraj, B. (2023). Experimental investigation on the performance of a pyramid solar still for varying water depth, contaminated water temperature, and addition of circular fins. *International Journal of Renewable Energy Development*, 12(6), 1123–1130. <https://doi.org/10.14710/ijred.2023.57327>
29. Yuvaperiyasamy, M., Senthilkumar, N., & Deepanraj, B. (2023). Experimental and theoretical analysis of solar still with solar pond for enhancing the performance of sea water desalination. *Water Reuse. https://doi.org/10.2166/wrd.2023.102*